HHS Public Access

Author manuscript

Kidney Int. Author manuscript; available in PMC 2024 September 01.

Published in final edited form as:

Kidney Int. 2023 September ; 104(3): 611–616. doi:10.1016/j.kint.2023.05.027.

Novel ARPKD mouse model with near complete deletion of Polycystic Kidney and Hepatic Disease 1 (*Pkhd1*) genomic locus has multiple phenotypes but no renal cysts

Yu Ishimoto[1,5], **Luis F Menezes**[1,5,6], **Fang Zhou**[1], **Teruhiko Yoshida**[1], **Taishi Komori**[2], **Jiahe Qiu**[1], **Marian F Young**[2], **Huiyan Lu**[3], **Svetlana Potapova**[3], **Patricia Outeda**[4], **Terry Watnick**[4], **Gregory G Germino**[1,6]

[1]Kidney Disease Branch; National Institute of Diabetes and Digestive and Kidney Disease (NIDDK), National Institutes of Health (NIH), Bethesda, Maryland, USA

[2]Molecular Biology of Bones and Teeth Section, Department of Health and Human Services (DHHS), National Institutes of Dental and Craniofacial Research (NIDCR), National Institutes of Health (NIH), Bethesda, Maryland, USA

[3]Mouse Transgenic Core Facility, National Institute of Diabetes and Digestive and Kidney Diseases (NIDDK), National Institutes of Health (NIH), Bethesda, MD, USA

[4]University of Maryland School of Medicine, Division of Nephrology, Baltimore, Maryland, USA.

[5]These authors contributed equally to the study.

[6]**Correspondence:** Gregory G. Germino: Building 31, Room 9A52, 31 Center Dr., Bethesda, MD 20892. gregory.germino@nih.gov. Luis F. Menezes: Building 10, Room 8D12A, 10 Center Dr., Bethesda, MD 20892 luis.menezes@nih.gov.

Disclosure

All the authors declared no competing interests.

Supplementary Material

Supplementary file: pdf file containing the following:

Supplementary methods, legends and references.

Supplementary figure S1. No evidence of embryonic lethality in *Pkhd1*$^{del3\text{-}67/del3\text{-}67}$ mice.

Supplementary figure S2. Liver and kidney weights over time.

Supplementary figure S3. Representative kidney image segmentation and analysis.

Supplementary figure S4. snRNAseq analysis of *Pkhd1*$^{del3\text{-}67/del3\text{-}67}$ kidneys.

Supplementary figure S5. Liver phenotypes in *Pkhd1*$^{del3\text{-}67/del3\text{-}67}$ mice.

Supplementary figure S6. Additional phenotypes in *Pkhd1*$^{del3\text{-}67/del3\text{-}67}$ mice.

Supplementary figure S7. lncRNA deleted in *Pkhd1*$^{del3\text{-}67/del3\text{-}67}$ mice.

Additional supplementary material was deposited in figshare with the following identifiers:

10.6084/m9.figshare.22734191:

Supplementary Table S1. PCR primers

Supplementary Table S2. Kidney and body weights of mice in figures 1 and S2

Supplementary Table S3. Eye and body weights of mice in figures 2 and S6.

10.6084/m9.figshare.22720789:

Supplementary snRNAseq analysis.

10.6084/m9.figshare.22726670:

Supplementary set of all images and pipeline used for analysis in figure S3.

Keywords

gene expression; pediatric nephrology; animal model

Autosomal recessive polycystic kidney disease (ARPKD) is a pediatric hereditary disease with an incidence varying from 1/10,000 to 1/40,000 live births. Most cases result from mutations in *PKHD1*, a large gene that spans approximately 469kb[1,2] and which undergoes complex splicing. Its longest open reading frame is encoded within a 67-exon mRNA transcript of ~13kb which is translated into fibrocystin (FPC), a ciliary protein of 4074 amino acids. While the variable severity of ARPKD is not completely understood [3], it has been observed that patients with truncating mutations in both alleles often die in the neonatal period, suggesting that in less severely affected patients partially functioning FPC could offer some protection [3]

Pkhd1, the mouse orthologue, has similar properties: it is large, extending over approximately 500kb of genomic DNA, and is spliced into multiple transcripts. *Pkhd1* expression is highest in renal and biliary tubular structures and, at lower levels, in several other organs, including tissue-specific transcripts detected with single exon probes [1]. Multiple mouse models lacking *Pkhd1* exons have been developed, and while most develop liver cysts, a kidney phenotype is uncommon. Supposing that splice variants might protect against severe kidney disease, Bakeberg *et al* used probes against exons 3–13; 22–32 and 44–50 and identified three additional smaller variants of the main *Pkhd1* transcript expressed in mouse kidneys [4]. Insertion of a STOP cassette in intron 2 abolished expression of all main *Pkhd1* transcripts, but did not result in severely cystic kidneys, suggesting these variants were not responsible for disease attenuation [4]. This study, however, did not exclude that alternative transcripts lacking the probed exons or low-level expression of transcripts bypassing the STOP cassette could prevent kidney disease.

To definitively exclude these possibilities, we generated a definitive *Pkhd1* null allele by deleting the complete genomic region between exons 2 and the 3'UTR using a novel strategy (Figure 1a). We produced this >400kb deletion by taking advantage of two mouse lines we had previously generated: $Pkhd1^{flox3\text{-}4}$, with lox P sites flanking exons 3–4 [5]; and $Pkhd1^{flox67HA}$, with lox P sites flanking the last exon [6]. The lines were intentionally designed so that after Cre-mediated recombination, the remaining lox P sites were similarly oriented. We generated mice carrying the deleted *Pkhd1* alleles, $Pkhd1^{del3\text{-}4}$ and $Pkhd1^{del67}$, and crossed them to *Ddx4*-Cre mice, a transgenic strain that expresses Cre in germ cells undergoing meiosis [7].

Using this strategy, we obtained 10 heterozygous mice carrying the novel $Pkhd1^{del3\text{-}67}$ allele from five independent breeding pairs, an approximately 20% success rate (Supplementary Figure S1a). We verified by PCR that recombination had properly occurred by testing for the presence of exon 1 and the 3'UTR, absence of intervening exons, and presence of a novel bridging fragment in $Pkhd1^{del3\text{-}67}$ homozygotes (Supplementary Figure S1b and Supplementary Table S1). Finally, we did whole genome sequencing (WGS) of one mutant animal and confirmed absence of reads mapping to any of the *Pkhd1* exons in the deleted region and presence of reads that mapped to both sides of the deletion region (Figure 1b).

Pkhd1$^{del3\text{-}67/del3\text{-}67}$ mice in this model were born healthy at expected mendelian ratios and had no perinatal lethality (Supplementary Figure S1c). Histological analysis of *Pkhd1*$^{del3\text{-}67/del3\text{-}67}$ mice revealed normal tubules and glomeruli, with no evidence of dilatation or cyst formation in collecting ducts in mice analyzed at various ages from birth to 15 months (Figure 1c). However, kidney weight / body weight (KW/BW) plots of our cohort of mice suggest that female *Pkhd1*$^{del3\text{-}67/del3\text{-}67}$ may have slightly larger kidneys compared to controls (Figure 1d, Supplementary Figure S2a, S2b and Supplementary Table S2). This finding is consistent with a previous report of histological dilatations in macroscopically normal *Pkhd1*$^{del3\text{-}4/del3\text{-}4}$ kidneys [5] and with a previous report showing mild kidney dilatation only in females of a truncating *Pkhd1* model [8]. Given a prior report of altered planar polarity in phenotypically normal *Pkhd1* mutant kidneys [9], we compared tubule diameter and cell number on cross sections of male and female mutant and wild type kidneys and found no difference (Supplementary Figure S3a–d; data in 10.6084/m9.figshare.22726670). We hypothesized that compensatory pathways might prevent cystogenesis in certain genetic backgrounds or environmental conditions, so we performed single nucleus transcriptomic studies of *Pkhd1* mutant and control kidneys and identified differentially expressed genes but no evidence for functional pathway abnormalities (Supplementary Figure S4a–e and supplementary analysis in 10.6084/m9.figshare.22720789). Network analysis suggests ubiquitin-conjugation may be altered (Supplementary Figure S4f).

Why complete *Pkhd1* deletion is insufficient to produce an ARPKD kidney phenotype in mice remains unclear. The *Pkhd1*$^{del3\text{-}67}$ line is derived from *Pkhd1*$^{del3\text{-}4}$, a model that initially had perinatal lethality and significant kidney disease. These phenotypes disappeared after selective breeding of survivors [5], suggesting that genetic modifiers likely account for much of the protection. There is strong evidence that multiple loci can influence disease expression in other rodent models and possibly in humans as well [10]. We predict that under appropriate genetic or environmental stressors *Pkhd1*$^{del3\text{-}67}$ could develop kidney cysts, and a true null model such as this provides a simpler platform for discovery since alternative *Pkhd1* transcripts are excluded as factors.

ARPKD also presents with a spectrum of liver phenotypes including biliary cysts, choledochal cysts, and ascending cholangitis [11] which have been nearly universal features of all previously reported *Pkhd1* mouse mutants. We observed all these phenotypes in *Pkhd1*$^{del3\text{-}67}$ homozygotes (Figure 1e, Supplementary Figure S5). Livers of newborn *Pkhd1*$^{del3\text{-}67/del3\text{-}67}$ mice were macroscopically normal but had an increased number of biliary cells. Macroscopic liver cysts were invariably present by 4 weeks of age, and liver disease worsened with aging (Supplementary Figure S5c). Mutant livers appear to properly form major branches of the biliary system with apparent diminished density of secondary branches (Figure 1f). Common bile duct dilatation and hypersplenism were commonly observed while pancreatic cysts and ascites were uncommon (Supplementary Figure S5f–i).

Quite unexpectedly, *Pkhd1*$^{del3\text{-}67/del3\text{-}67}$ mutants have several other problems. All mutant mice developed corneal opacities (Figure 2a) in one or both eyes detectable within the first 3–4 weeks of life, often accompanied by changes in eye globe size (Figure 2b, Supplementary Figure S6a–c and Supplementary Table S3). The phenotype progressively

worsened with age, became invariably bilateral and sometimes resulted in corneal ulcerations requiring euthanasia. Approximately 80% of the mutants also developed malocclusion due to misaligned incisors (Figure 2c, 2d), a phenotype very rarely observed in controls or other mutant lines[12]. Teeth number and other facial features appeared normal. Analysis of the TMJ condyles from *Pkhd1*$^{del3\text{-}67/del3\text{-}67}$ showed they did not have significant changes in their shape; however, they had reduced subchondral Bone Volume/Tissue Volume (BV/TV) (Supplementary Figure S6d, S6e). While eye and orofacial abnormalities have been described in other ciliary mutants[13 14] and FPC is a ciliary protein, these phenotypes have not been reported associated with human ARPKD or in other *Pkhd1* mutant rodent models. We think deletion of regulatory elements within the *Pkhd1* locus that disrupt expression of other genes and/or loss of a long non-coding RNA embedded within the *Pkhd1* locus (described below) are more likely explanations.

While expanding the *Pkhd1*$^{del3\text{-}67}$ mouse line, we frequently observed small litter sizes when using male homozygotes as sires. We therefore performed a series of *in vitro* fertilization (IVF) procedures using harvested sperm from adult male *Pkhd1*$^{del3\text{-}67}$homozygotes and littermate controls and found that mutant sperm fertilized eggs at much lower IVF rates than controls (Figure 2e). A review of our records confirmed that the problem had already been present years earlier, when we performed *in vitro* fertilization using several *Pkhd1* mutant lines and controls and observed low rates only in the *Pkhd1*$^{del3\text{-}67}$ line. These observations suggest that reduced fertility is a unique feature of the *Pkhd1*$^{del3\text{-}67}$ line.

Though detailed characterization of this phenotype is beyond the scope of this study, it is notable that we had previously found a highly expressed ~1.0kb mRNA transcript in testis that was detected with an exon 41 probe and not with one from exon 5 [1]. In an RNA-seq dataset from mouse testis, we found several reads in the *Pkhd1* locus in all cell types, but reads only aligned to exons spanning the whole *Pkhd1* gene in the differentiated spermatogonia (Supplementary Figure S7). In other cell types, the reads predominantly mapped to exons of *4930486I03Rik,* a long non-coding RNA of unknown function embedded within *Pkhd1.* The gene is in the opposite orientation to *Pkhd1* and its third exon overlaps with *Pkhd1*'s exon 38 (Figure 2f) and is highly expressed in testis (Figure 2g). *Pkhd1* and *4930486I03Rik* have mostly overlapping patterns of tissue expression though there is an inverse relationship between their levels of expression, particularly in testis.

In summary, our studies show that *Pkhd1* alternative splicing does not explain the lack of cystic kidneys in ARPKD mouse models. The presence of unique phenotypes is this model suggests that deletion of the *Pkhd1* locus can have pathogenic effects in multiple organs, consistent with cell-type specific transcripts, deletion of yet uncharacterized genes in the genomic interval, and/or disruption of long-range chromosomal regulatory interactions. This model will be useful to understand these processes and *Pkhd1*'s role in them. Our approach can be also used more generally to efficiently induce novel intragenic alleles between pre-existing lox P sites.

Supplementary Material

Refer to Web version on PubMed Central for supplementary material.

Data sharing statement

Single nuclear RNA sequencing related datasets generated for this study can be found in the NCBI Sequence Read Archive (SRA) archive with BioProject record PRJNA911229. Cellrange output count matrices were deposisted in figshare with digital object identifier (DOI): <10.6084/m9.figshare.22726550>.

References

1. Nagasawa Y, Matthiesen S, Onuchic LF, et al. Identification and characterization of Pkhd1, the mouse orthologue of the human ARPKD gene. J Am Soc Nephrol. 2002;13(9):2246–2258. [PubMed: 12191969]
2. Ward CJ, Hogan MC, Rossetti S, et al. The gene mutated in autosomal recessive polycystic kidney disease encodes a large, receptor-like protein. Nat Genet. 2002;30(3):259–269. [PubMed: 11919560]
3. Rossetti S, Harris PC. Genotype-phenotype correlations in autosomal dominant and autosomal recessive polycystic kidney disease. J Am Soc Nephrol. 2007;18(5):1374–1380. [PubMed: 17429049]
4. Bakeberg JL, Tammachote R, Woollard JR, et al. Epitope-tagged Pkhd1 tracks the processing, secretion, and localization of fibrocystin. J Am Soc Nephrol. 2011;22(12):2266–2277. [PubMed: 22021705]
5. Garcia-Gonzalez MA, Menezes LF, Piontek KB, et al. Genetic interaction studies link autosomal dominant and recessive polycystic kidney disease in a common pathway. Hum Mol Genet. 2007;16(16):1940–1950. [PubMed: 17575307]
6. Outeda P, Menezes L, Hartung EA, et al. A novel model of autosomal recessive polycystic kidney questions the role of the fibrocystin C-terminus in disease mechanism. Kidney Int. 2017;92(5):1130–1144. [PubMed: 28729032]
7. Gallardo T, Shirley L, John GB, Castrillon DH. Generation of a germ cell-specific mouse transgenic Cre line, Vasa-Cre. Genesis. 2007;45(6):413–417. [PubMed: 17551945]
8. Shan D, Rezonzew G, Mullen S, et al. Heterozygous Pkhd1(C642*) mice develop cystic liver disease and proximal tubule ectasia that mimics radiographic signs of medullary sponge kidney. Am J Physiol Renal Physiol. 2019;316(3):F463–f472. [PubMed: 30600684]
9. Nishio S, Tian X, Gallagher AR, et al. Loss of oriented cell division does not initiate cyst formation. J Am Soc Nephrol. 2010;21(2):295–302. [PubMed: 19959710]
10. Guay-Woodford LM. Murine models of polycystic kidney disease: molecular and therapeutic insights. Am J Physiol Renal Physiol. 2003;285(6):F1034–1049. [PubMed: 14600027]
11. Zerres K, Rudnik-Schöneborn S, Deget F, et al. Autosomal recessive polycystic kidney disease in 115 children: clinical presentation, course and influence of gender. Arbeitsgemeinschaft für Pädiatrische, Nephrologie. Acta Paediatr. 1996;85(4):437–445. [PubMed: 8740301]
12. Boily G, He XH, Jardine K, McBurney MW. Disruption of Igfbp1 fails to rescue the phenotype of Sirt1−/− mice. Exp Cell Res. 2010;316(13):2189–2193. [PubMed: 20412791]
13. Portal C, Rompolas P, Lwigale P, Iomini C. Primary cilia deficiency in neural crest cells models anterior segment dysgenesis in mouse. Elife. 2019;8.
14. Brugmann SA, Cordero DR, Helms JA. Craniofacial ciliopathies: A new classification for craniofacial disorders. Am J Med Genet A. 2010;152A(12):2995–3006. [PubMed: 21108387]

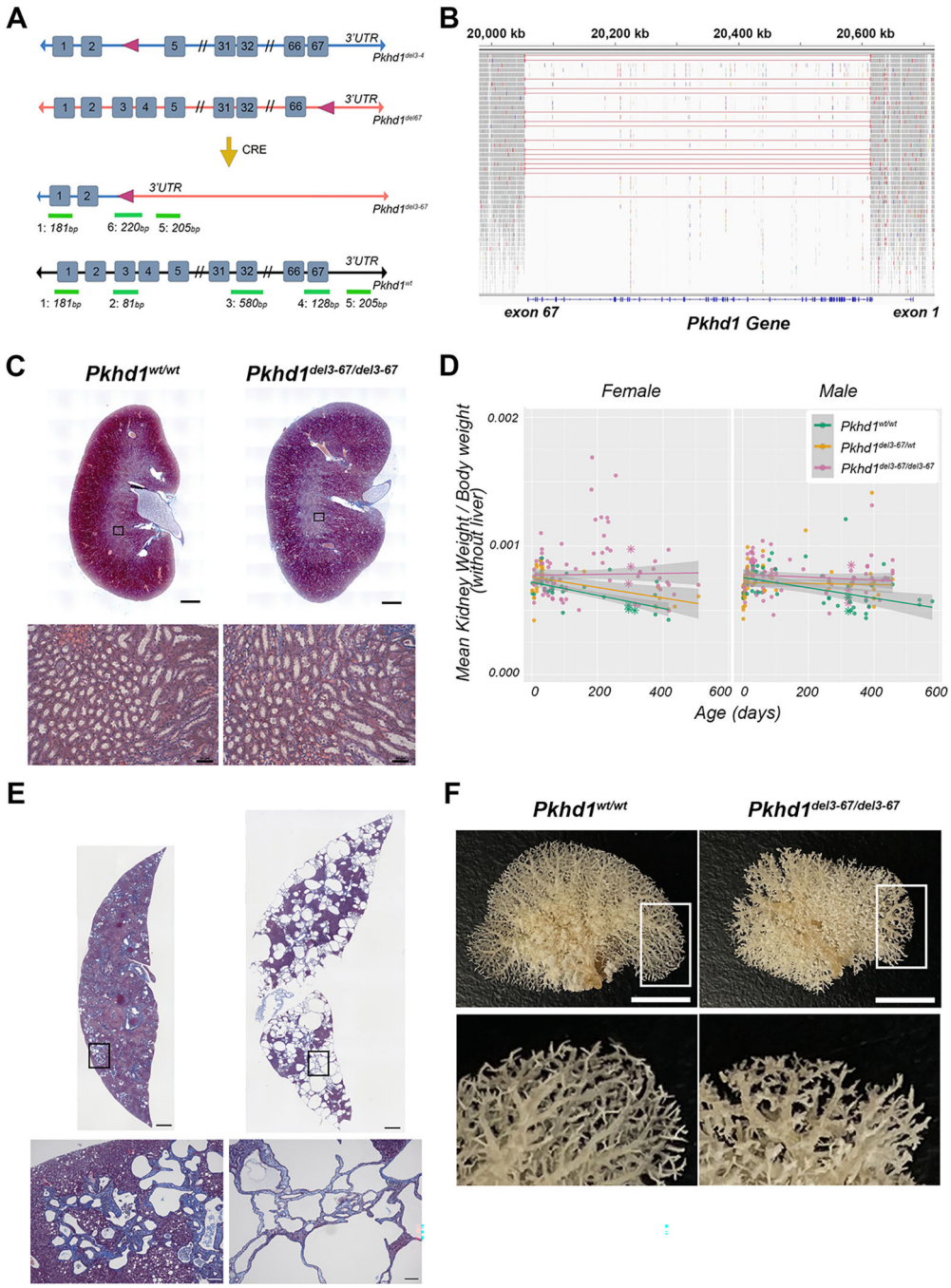

Figure 1 |. Generation of *Pkhd1*$^{del3-67}$ mouse and phenotypes in the kidney and liver.

(a) Generation of *Pkhd1*$^{del3-67}$ allele. We bred mice carrying 2 *Pkhd1* alleles *Pkhd1*$^{del3-4}$ and *Pkhd1*^{del67} and with embryonic germ cell transgenic expression of Cre recombinase. In some pups, interchromosomal recombination of the *Pkhd1* alleles resulted in deletion of exons 3 to 67 (numbered boxes: exons; purple arrowhead: lox P sites; green/white rectangles mark predicted polymerase chain reaction [PCR] products and sizes in both wild-type and mutant *Pkhd1* alleles). **(b)** Whole genome sequence showing the *Pkhd1* region in a mutant *pkhd1*$^{del3-67/del3-67}$ mouse, visualized using Integrative Genomics Viewer.[6] The vertical

bars correspond to individual reads. The horizontal red lines correspond to reads that map to both sides of the deletion region. Note the absence of reads in *Pkhd1* exons in the predicted deleted region. **(c)** Masson's trichrome staining of the kidneys of wild-type (wt) and *pkhd1*$^{del3\text{-}67/del3\text{-}67}$ mice. Upper panel: Whole kidney images of 457-day-old littermates. Bar = 1000 μm. Lower panel: Higher magnification of microscopic images of collecting ducts. Bar = 50 μm. **(d)** Graphs of kidney weight/body weight (excluding liver weight) ratio (Y axis) over time (X axis; mouse age in days). Left panel: Females. Right panel: Males. Gray areas show the 95% confidence interval. Dots represented by asterisks were used for pathological analysis for Supplementary Figure S3. Two of the male wt samples had nearly identical values and not distinguishable, **(e)** Representative liver images of 15-month-old *pkhd1*$^{del3\text{-}67/del3\text{-}67}$ mice, showing the range in the degree of cystic change and fibrosis (Masson's trichrome staining). Upper panel: Whole liver images. Bars = 1000 μm. Lower panel: Higher magnification of area highlighted in the upper panel. Bars = 100 μm. **(f)** Three-dimensional resin casting of the biliary system of 2-month-old wt and *pkhd1*$^{del3\text{-}67/del3\text{-}67}$ littermates (left lobe). Top panel: Whole liver images. Bars = 5 mm. Bottom panels: Boxed areas at higher magnification. *Pkhd1,* polycystic kidney and hepatic disease 1; UTR, untranslated region. To optimize viewing of this image, please see the online version of this article at www.kidney-international.org.

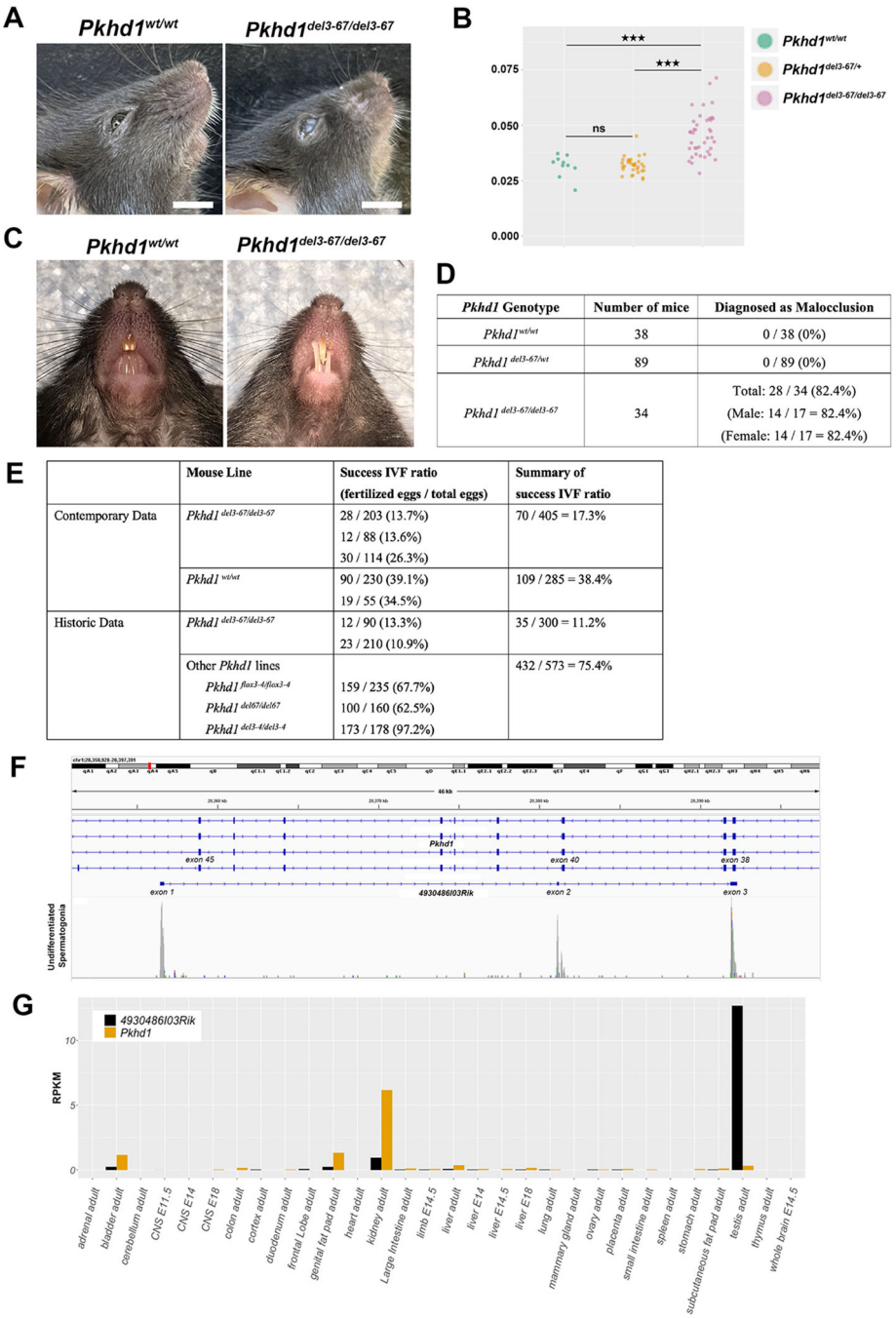

D

Pkhd1 Genotype	Number of mice	Diagnosed as Malocclusion
Pkhd1 wt/wt	38	0 / 38 (0%)
Pkhd1 del3-67/wt	89	0 / 89 (0%)
Pkhd1 del3-67/del3-67	34	Total: 28 / 34 (82.4%) (Male: 14 / 17 = 82.4%) (Female: 14 / 17 = 82.4%)

E

	Mouse Line	Success IVF ratio (fertilized eggs / total eggs)	Summary of success IVF ratio
Contemporary Data	*Pkhd1* del3-67/del3-67	28 / 203 (13.7%) 12 / 88 (13.6%) 30 / 114 (26.3%)	70 / 405 = 17.3%
	Pkhd1 wt/wt	90 / 230 (39.1%) 19 / 55 (34.5%)	109 / 285 = 38.4%
Historic Data	*Pkhd1* del3-67/del3-67	12 / 90 (13.3%) 23 / 210 (10.9%)	35 / 300 = 11.2%
	Other *Pkhd1* lines		432 / 573 = 75.4%
	Pkhd1 flox3-4/flox3-4	159 / 235 (67.7%)	
	Pkhd1 del67/del67	100 / 160 (62.5%)	
	Pkhd1 del3-4/del3-4	173 / 178 (97.2%)	

Figure 2 |. Unexpected phenotypes of *pkhd1*$^{del3\text{-}67/del3\text{-}67}$ mice.

(a) Representative images of eyes from control and mutant 100-day-old mice. Only *pkhd1*$^{del3\text{-}67/del3\text{-}67}$ mice develop corneal opacities. Bars = 50 mm. **(b)** Eye weight of 4-week-old mice. Each dot indicates the combined weight of the left and right eyes per mouse. $^{***}P < 0.0001$ **(c)** Representative image of malocclusion in 2-month-old *pkhd1*$^{del3\text{-}67/del3\text{-}67}$ mouse (right) and its littermate control (left). **(d)** Rates of incisor malocclusion. **(e)** Summary of *in vitro* fertilization (IVF) results for *Pkhd1* mutant mouse lines. **(f)** Visualization of the genomic region including *Pkhd1* exons 38–45 and

4930486103Rik exons 1–3. The peaks at the bottom represent the number of reads identified in undifferentiated spermatogonia. Data were obtained from GSE162740. **(g)** Data from published databases showing *4930486103Rik* transcript abundance in various organs. The highest expression of *4930486103Rik* is in testis. NS, not significant; *Pkhd1,* polycystic kidney and hepatic disease 1; RPKM, reads per kilobase per million reads; wt, wild type.